Femtosecond Dynamics of Piroxicam Structures in Solutions

Michał Gil and Abderrazzak Douhal*

Departamento de Química Física, Sección de Químicas, Facultad de Ciencias del Medio Ambiente, Universidad de Castilla-La Mancha, Avenida Carlos III, S.N., 45071, Toledo, Spain

Received: April 21, 2008; Revised Manuscript Received: July 8, 2008

We report on studies of femtosecond dynamics of a nonsteroidal anti-inflammatory drug, piroxicam (**1**), in water at three different pHs and for comparison in two aprotic solvents. An ultrafast excited-state proton-transfer (ESIPT) process takes place in neutral and cationic enol-type structures. Femtosecond emission and transient absorption experiments show that this reaction is barrierless, and the proton-transferred keto tautomer is formed in less than 100 fs in both organic solvents and acidic water. In neutral and alkaline water, the ESIPT is not present because of the prevalence of the anion structures at the ground state. For the excited anions (pH = 7, 11) and formed keto cations (pH ≈ 3), an intramolecular charge-transfer process takes place in times shorter than 0.3 ps. The formed structures have a fluorescence lifetime of ∼2−5 ps, depending on pH. In contrast, the internal twisting motion in organic solvents is slower (∼0.5−1 ps) and gives rotamers with lifetimes of tens of picoseconds. These results clearly show strong interactions of **1** with water, significantly distinct from those present in organic aprotic solvents. We believe that the results are important for a better understanding on short time interactions of drugs with their environment.

1. Introduction

Over the last two decades, interest in studying photophysical properties of several classes of drugs has grown continuously.[1−8] Recent progress in ultrafast spectroscopy provided new tools to investigate the very first events occurring after photon absorption.[9,10] Knowledge about light-induced processes and excited-state reactions is no longer limited to conventional examination of final products, but detailed relaxation pathways and reaction timing are accessible. In addition to the insight into fundamental scientific problems (e.g., proton transfer or isomerism), the obtained data could be useful for a better drug design or in resolving practical issues such as storage photostability or phototoxicity of drugs. The latter can be especially important for the widely used group of nonsteroidal anti-inflammatory drugs (NSAID), which are known for some unwanted biological photoactivity.[11,12]

Piroxicam (**1**) belongs to a less photoactive group of NSAID. It can exist in several prototropic forms (Figure 1).[13,14] The spectral properties of **1** in different solvents were investigated by steady-state UV−visible absorption and emission spectroscopy.[15−18] The positions of maxima in intensity of absorption and emission spectra depend on hydrogen-bonding abilities of solvent. In aprotic and nonpolar solvents, the absorption is due to the enol (**1a**) form with an intramolecular H-bonding between the OH and the ortho carbonyl groups of the benzothiazine ring.[15] The maximum of emission is observed at ∼480 nm with a large Stokes shift of ∼9000 cm^{-1}.[15] The abnormal shift is explained by the presence of an excited-state intramolecular proton-transfer (ESIPT) process at S_1 in **1a** leading to a keto-type tautomer (**1b**).[15] In alcohols, a dual fluorescence was observed with maxima of intensity depending on the excitation wavelength.[15,16] In addition to the tautomeric emission, the weak normal fluorescence was detected at ∼400 nm. The latter was suggested to be due to an open conformer (without intramolecular H-bond) or an anionic (**1c**) form.[17] The ESIPT process to form excited **1b** and solvent-mediated ground-state formation of anion depend strongly on the concentration of the drug in alcohols.[18] At a high concentration of **1** (10^{-4} to 10^{-2} M), the ESIPT is the dominant process, whereas at the low concentration the excited-state conformational change of anion to a zwitterionic (**1d**) form was observed.[18]

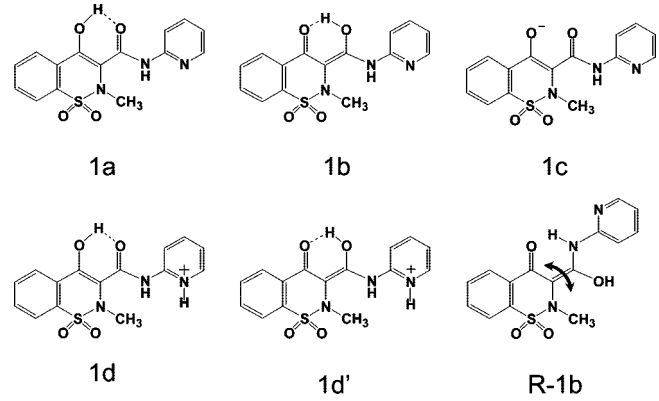

Figure 1. Structures of piroxicam (**1**): enol (**1a**), keto (**1b**), anionic (**1c**), cationic (**1d**), keto cationic (**1d′**) forms, and one possible rotamer of keto structure (**R-1b**).

Solvent dependence of tautomerism of **1** has been also studied.[19−21] A correlation of solvent hydrogen donor capacity with the dominant form of **1** in solution has been reported.[19] It suggests that in protic solvents the open conformer with intermolecular H-bond prevails, but the closed enol form also exists. The coexistence of anionic form of **1** has not been excluded, as suggested by a very low pK_a value of the phenol part.[19] In pure water at pH ≈ 7, the anionic form has been suggested to predominate in addition to open conformer and the closed one.[20,21] The formation of anion absorption band with maximum at ∼360 nm in ethylene glycol at low concentration (∼10^{-6} M) of the drug has been shown recently.[22]

* Corresponding author. Fax: +34-925-268840. E-mail: Abderrazzak.douhal@uclm.es.

10.1021/jp803457e CCC: $40.75
Published on Web 08/15/2008

Being a drug, piroxicam has been studied in various heterogeneous media, such as cyclodextrins (CD), reversed micelles, and human serum albumin (HSA) protein. For aqueous CD solutions, it has been shown that neutral species of **1** form a 1:1 complex through the benzothiazine part of the molecule.[17,23] The ESIPT emission is allowed, and it is attributed to the hydrophobicity of the CD cavity. This leads to increased inclusion of intramolecularly hydrogen-bonded enol tautomer **1a** by converting the anionic form into an encapsulated neutral one.[17,22,23] The spectroscopic behavior of **1** in reverse micelles is similar to the one observed in β-CD. The equilibrium between neutral and anionic forms has been found very sensitive to water content and pH of the environment.[20,21,24] At pH = 4, the neutral form of the drug is preferentially located in the interfacial region between hydrophobic and hydrophilic domains, whereas at pH = 7, the anionic species is prevalent and is deeper inside the water core of the reversed micelle.[21] These findings reflect the sensitivity of the drug to traces of water in both protic and aprotic solvents.[16]

Studies of the interactions between piroxicam and HSA protein have shown spontaneous complex formation.[22,25,26] These interactions involve H-bonding and hydrophobic forces between the drug and the protein pocket.[25,26] It has been suggested that the anionic form preferentially binds to site I in subdomain IIA, and the zwitterionic one binds to site II in subdomain IIIA.[22] The complex is not completely rigid, and diffusive motion of the drug inside the HSA pocket takes place with a rotational time of ~170 ps.[22] Energy transfer between the excited tryptophan of HSA protein and the encapsulated drug (anion or enol) takes place with 50% of efficiency.[22]

Time-resolved spectroscopy is a powerful tool to investigate conformational changes in organic molecules. Several works involved these methods for studying tautomerism in **1**.[15,17,21,22,27,28] For aprotic solutions, times of ~50−60 ps have been assigned to the emission lifetimes of relaxed keto tautomers and their rotamers formed after an ultrafast ESIPT (in less than 100 fs).[15,21,22,27] The formation of twisted structures takes place in ~2−5 ps, depending on the viscosity of solvent.[28] The latter parameter affects also nonradiative deactivation of **1**, increasing its lifetime in triacetin (viscosity η_{298K} = 17 cP) to 155 ps.[28] On the other hand, the fluorescence lifetime of **1** in neutral and alkaline water has been found to be shorter than 10 ps.[17,21,22] It originates from anionic species, which has also a very low fluorescence quantum yield in this media. In addition to this time constant, another component in nanosecond time scale has been detected, although its contribution in the emission signal is very small.[17,21,22] This component was attributed to an open conformer with intermolecular hydrogen bonding of **1** to water molecules.

Laser flash photolysis has been used to examine triplet states of enol form of **1**.[29] The maximum of triplet transient absorption spectrum is at ~450 nm, and the triplet lifetime of 3−21 μs depends on the solvent. The relative quantum yield of triplet formation has been found highly solvent dependent with maximum in toluene and minimum in hydrogen-bonding solvents.[29] Also, a direct observation of the triplet state of keto tautomer in toluene with lifetime of 7.5 ns has been reported.[27]

Therefore, **1** has been studied in several media using different techniques. However, to the best of our knowledge, there is no study of **1** in water solutions using femtosecond spectroscopy to observe the early stages of structure conversion and formation. In this work, we continue our efforts in this direction to provide a detailed picture of the relaxation dynamics of piroxicam. Recent reports from this group revealed the presence of very fast components in the dynamics of piroxicam in organic solutions, much faster than the previously reported one.[22,27,28] Here, we observed large differences in the femtosecond dynamics of neutral and ionic forms of **1**. The result is explained in terms of ultrafast proton-transfer, twisting motion, and charge-transfer processes occurring after UV light excitation of the most stable structure, which strongly depends on the nature of the medium.

TABLE 1: Time Constants (τ_i) and Normalized (to 1) Pre-exponential Factors (a_i) of the Functions Used in Fitting the Femtosecond Emission Transients of 1 in THF at Different Wavelengths of Observation (λ_{obs}), upon Excitation at 377 nm[a]

λ_{obs}/nm	τ_1/fs	a_1	τ_2/ps	a_2	τ_3/ps	a_3
410	130	0.84	1.8	0.10	45	0.06
445	210	0.47	2.0	0.23	45	0.30
463	290	0.38	2.4	0.19	45	0.43
481	290	0.25	2.2	0.17	45	0.58
500	290	0.25	3.9	0.13	45	0.62
530			3.1	0.08	45	0.92
550					45	1.00
580			0.9	−0.14	45	0.86
610			1.0	−0.16	45	0.84
640			1.3	−0.19	45	0.81
660			1.4	−0.21	45	0.79

[a] The sign (−) in a_2 indicates a rising component.

2. Experimental Section

Piroxicam (1,2-benzothiazine-3-carboxamide-4-hydroxy-2-methyl-*N*-(2-pyridyl)-1,1-dioxide; 98%, Sigma-Aldrich) and spectroscopic-grade solvents (Sigma-Aldrich) were used as received. We used a buffer of 50 mM sodium phosphate in Milli-Q water giving a pH = 7. The pH of the acidic (pH = 3) and alkaline (pH = 11) solutions was adjusted by adding aliquots of HCl and NaOH water solutions. We did not observe any evidence of aggregation, stacking, or crystal precipitation during experiments.

The femtosecond emission transients were recorded using fluorescence up-conversion system.[30] It consists of a femtosecond Ti:sapphire oscillator (Tissa 100) coupled to an up-conversion setup. The pulses (70 fs, 500 mW) were centered at 760 nm (or 780 nm), with 86 MHz repetition rate and doubled (or tripled) in an optical setup containing BBO crystals (0.5 mm) to have a pumping beam at 377 or 261 nm (0.1−0.5 nJ, at 86 MHz). The polarization of the latter was rotated at magic angle in respect to fundamental beam. Fluorescence from a 1-mm-thick, rotating cell was focused with reflective optics to a 0.5-mm BBO. The typical instrument response function (IRF) of the apparatus was ~180 fs with excitation at 377 nm, or ~390 fs with excitation at 261 nm. The time-resolved emission spectra (TRES) were constructed with use of the data from Table 1. Steady-state UV−visible absorption and emission spectra were recorded on Carry 1E (Varian) and Perkin-Elmer (LS 50B) spectrophotometers, respectively.

The time-resolved UV−visible transient absorption spectra and kinetics were collected using a two-channel femtosecond apparatus.[28] Briefly, pulses (30 fs, 450 mW at 86 MHz repetition rate) from the Ti:sapphire laser centered at 800-nm wavelength were amplified (50 fs, 1 W at 1 kHz repetition) and doubled (or tripled) in an optical system containing BBO crystals to have a pumping beam centered at 400 nm (or 267 nm). The remaining fundamental beam generated a white light continuum in a 1-mm cell with flowing water. The produced white light formed probe

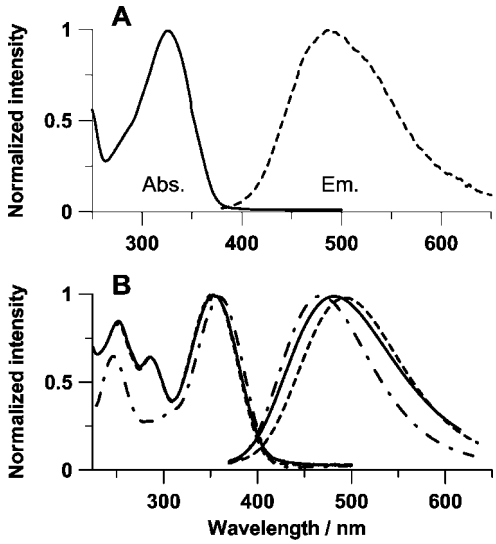

Figure 2. Normalized UV−visible absorption (Abs) and emission (Em) spectra of **1** in (A) THF and (B) water solutions at pH = 3 (− • −), 7 (−), and 11 (− − −).

and reference beams, which passed through a rotating 1-mm-thick cell containing the sample. Both beams were then directed to a spectrograph and collected by a pair of photodiode arrays (1024 elements, for spectral measurements) or by a pair of avalanche photodiodes (decays). Polarization of the pumping beam was set to magic angle in respect to the probe. The IRF of the apparatus was ∼450 fs, and in some case ∼380 fs.

Multiexponential functions convoluted with the IRF signal were fitted to the kinetic traces of emission and absorption using the Fluofit software. All measurements were done at 293 ± 1 K, and the concentration of the sample in the femtosecond experiment was $\sim 10^{-3}$ M.

3. Results and Discussion

3.1. Steady-State Observation. Figure 2 shows steady-state UV−visible absorption and emission spectra of **1** in tetrahydrofuran (THF) and in water at three different pH values. In THF, the maximum in intensity of absorption band is at 326 nm, which suggests the prevalence of enol form of **1** at the ground state (S_0). The fluorescence spectrum has its maximum of intensity at 485 nm. It gives a large Stokes shift of ∼10 000 cm^{-1}, and it indicates the occurrence of an ESIPT process leading to keto-type structures. We observed a similar behavior in acetonitrile (not shown), a more polar solvent. Recent experiments in solution and upon encapsulation into a cyclodextrin cavity show that after the ESIPT an internal twisting motion happens at S_1 in 2−5 ps, generating rotamer structures of **1b**.[22,28]

In water, the absorption spectra at pH = 7 and 11 (Figure 2B) are nearly identical, having their maximum of intensity at 355 nm. However, the emission spectrum recorded at pH = 11 is shifted to longer wavelengths (494 nm) in respect to that obtained at neutral pH (482 nm). The red shift of the emission maximum at pH = 11 when compared to that at pH = 7 is explained in terms of a different solvation of the anion in an alkaline water solution or by the presence of different structures having different contribution (population) at the excited states in these media. The related structures are shown in Figure 1 and according to previous contributions.[17−22] The femtosecond dynamics (vide infra) will give more information.

At pH = 3, the absorption spectrum has the maximum of the first transition slightly shifted to the red side (359 nm). The second band is absent in comparison with other pHs, which indicates a different form of **1** at this pH. The pK_a value for a protonation of piridyl nitrogen site is ∼5. Thus, at pH ≈ 3, the cation (**1d**) form of the drug at the ground state is the dominant structure. We did not notice any dependence of absorption spectrum on concentration of the drug. The maximum of emission appears at this pH value at 467 nm.

3.2. Femtosecond Time-Resolved Emission Observations. Our previous work on **1** in water solutions revealed the presence of a very fast (<10 ps) component in the picosecond fluorescence decays. Therefore, we studied the femtosecond dynamics of **1** by gating its time-resolved emission and absorption spectra and transients.

Table 1 shows the parameters (time constants and relative amplitudes) obtained from a multiexponential fit of femtosecond emission transients recorded in THF upon excitation at 377 nm. (Experimental signals collected at various observation wavelengths together with fitted curves are presented as Supporting Information, Figure S1.) Within the gated emission wavelengths, we identified three families of transients. The first one (I) consists of decay curves observed from the high-energy part to the maximum of the band (400−500 nm). A three-exponential function was used to fit the transients, and the obtained time constants are τ_1 = 130−290 fs, τ_2 = 1.8−3.9 ps, and τ_3 = 45 ps (Table 1). The shortest component has the maximum of its amplitude at the high-energy side of the spectrum. Intramolecular vibrational-energy redistribution takes place in this time scale. Its contribution is more pronounced at higher-energy side. A proton-transfer reaction time in this region normally appears as a rising component, which excludes the assignment the femtosecond component to the ESIPT reaction in **1a**. The occurrence of this event appears as an unresolved rise of the transient at the blue region (∼400−420 nm). The intermediate component (∼2−4 ps) has a relatively small amplitude (0.1−0.2), but it is observed up to 530 nm. We associate this time constant with vibrational relaxation (VR)/cooling processes taking place after ultrafast ESIPT and with twisting motion process around C−N or C−C single bonds, as we have recently shown in other solvents.[28] The longest component (∼45 ps), obtained from a large time window (400 ps) experiment was fixed in the fit. Its value is in agreement with a previously measured one in a picosecond apparatus, and it is attributed to the lifetime of relaxed keto rotamers formed after twisting motion in the photoproduced keto tautomer.[22] Several conformers of this rotamer are possible after twisting around C−C and/or C−N bonds, connecting both aromatic parts of the molecule. One of them is schematically shown in Figure 1 (structure **R-1b**).

The second family of transients at the region around 550 nm consists of single-exponential decays. Most probably, the signal is affected by the decaying and rising components of regions I and III, respectively.

The third family represents transients at the red part of stationary emission band (580−660 nm). In addition to the long-lived decaying component, we observed a rising time constant. A value of ∼1−1.4 ps and a growing amplitude with wavelength of observation were obtained (Table 1). The presence of a picosecond component decaying at the blue side and rising at the red one suggests that the related time is for the production of rotamers of **1b**, in agreement with our previous report in other solvents.[28] Furthermore, this explanation is supported by TRES shown in Figure 3. The emission spectrum gated at 50 fs has its maximum in intensity at 465 nm, and its band is extended to shorter wavelengths. This suggests that this signal

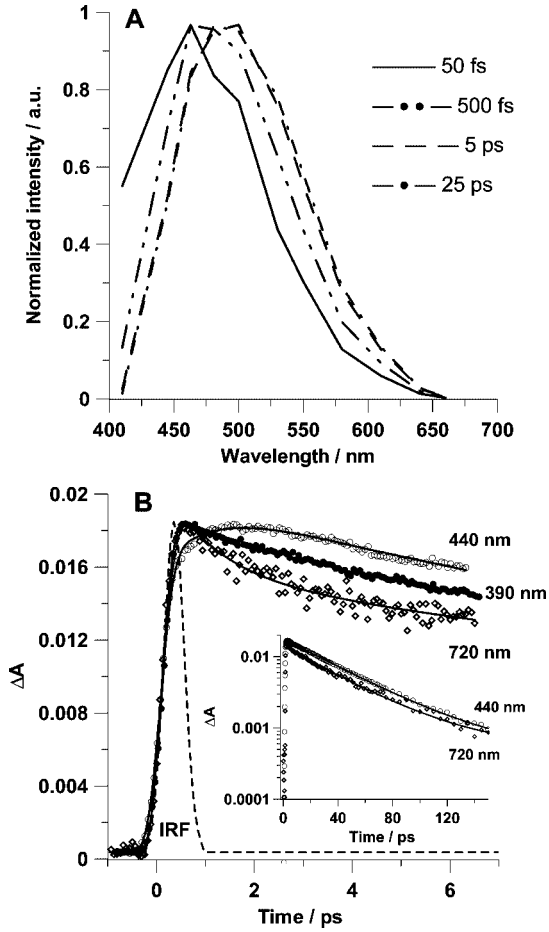

Figure 3. (A) Normalized TRES of **1** in THF at pump−probe delays: 50 fs, 0.5 ps, 5 ps, and 25 ps. The excitation wavelength was 377 nm. (B) Transient absorption decays of **1** in THF observed at 390, 440, and 720 nm. The solid lines are from multiexponential fits (see Table 2 for details), and the dashed line is the IRF signal. The inset shows 440- and 720-nm decays for a longer window of observation.

is mainly coming from the initially formed keto tautomers after an ultrafast (<50 fs) ESIPT reaction in excited **1a**. The 500-fs gated spectrum shifts to longer wavelength, and this behavior is more pronounced for the 5-ps spectrum. At longer times, we observed no further change in position and shape of the spectrum. Notice that the rising times obtained in region III are smaller than the corresponding decay values of region I. This is because we used a two-exponential model for the analysis of the transients at the red part of the spectrum. An attempt to use a third rising component in the fitting procedure gave times very similar to those obtained at the blue side (i.e., ∼200 fs and ∼2 ps). However, the difference in the quality of the fit was not high enough to justify the use of a three-exponential model.

To study if the excess of excitation energy influences the relaxation dynamics of **1**, we pumped the drug at 261 nm. We found a behavior similar to the one described for 377-nm excitation (Supporting Information, Table S1 and Figure S2). The obtained times are slightly longer at comparable wavelengths of observation (200−300 fs and 2.7−3.8 ps for first and second component, respectively), but the pumping energy does not influence significantly the measured dynamics. This result indicates that the proton-transfer process takes place at the locally excited enol form (with or without excess energy of excitation). It is essentially barrierless, and the evolution of the keto structure toward the keto rotamers occurs after an instantaneous relaxation into their potential energy surfaces (PES).

TABLE 2: Time Constants (τ_i) and Normalized (to 1) Pre-exponential Factors (a_i) of the Transient Absorption and Stimulated Emission Decays of 1 in THF and ACN Solutions at Different Wavelengths of Observation, upon Pumping at 267 nm[a]

medium	λ/nm	τ_1/ps	a_1	τ_2/ps	a_2	τ_3/ps	a_3
THF	390			3	0.17	41	0.83
	440	0.9	−0.22			42	0.78
	560	0.9	0.13			45	0.87
	720	1.0	0.25			42	0.75
ACN	390			3	0.10	27	0.90
	440	0.5	−0.31	3	0.19	27	0.50
	540	0.9	0.38			27	0.62
	720	0.5	0.26			27	0.74

[a] The sign (−) in a_1 indicates a rising component.

3.3. Femtosecond Time-Resolved Absorption in Aprotic Solvents. The transient absorption spectra obtained in THF are similar in shape to those previously shown for methyl acetate.[28] They have two positive maxima in intensity at ∼430 and 740 nm, while a minimum with a negative intensity is around 540 nm (Supporting Information, Figure S3). The latter comes from a stimulated emission of keto rotamers. The higher-energy part of the band (390−500-nm region) is different from the previously reported transient absorption in toluene, assigned to a triplet state decaying on a nanosecond time scale.[27] The reason for the spectral difference is that we are probing the S_1 dynamics after an ESIPT reaction in **1** in THF. The broad transient absorption band reflects that the excited-state PES is relatively flat at S_1 after the proton motion. This shows the large sensitivity of the drug to properties of environment, such as a viscosity and proticity of solvent. Recently, we showed how the barrier for internal rotation in **1b** can be modified by friction with a viscous solvent.[28]

Figure 3B gives representative decay curves of transient absorption in THF at three different regions, and Table 2 gives the data of multiexponential fits. Three components are present giving times of $\tau_1 \approx 1$ ps, $\tau_2 \approx 3$ ps, and $\tau_3 \approx 42$ ps. The ∼42-ps component corresponds to the lifetime of relaxed keto rotamers at S_1. The two other picosecond components attributed to the dynamics of keto and its rotamers were obtained at the high- and low-energy sides of the spectrum, where the stimulated emission is absent. The ultrafast (femtosecond) time constants measured in the femtosecond emission experiment do not manifest themselves in these transient absorption decays. Its absence is mostly due to the relatively lower temporal resolution of the transient absorption setup (IRF ≈ 450 fs) in comparison with the fluorescence up-conversion apparatus (IRF ≈ 180 fs). However, we observed the influence of these femtosecond processes on the obtained transient absorption components of ∼1 ps (at 720 nm) and 3 ps (at 390 nm), as they are slightly shorter than the related femtosecond emission values (which are between 1.8 ps and ∼4 ps for lower and higher energy of excitation, respectively). Similarly to the explanation of the data of femtosecond emission experiments, we assign the 1 ps to the twisting of **1b** to give its rotamer and 3 ps to a subsequent VR/cooling in this structure. At 560 nm, the transient signal is dominated by a stimulated emission. The obtained time constants (0.9 and 45 ps) are very similar to those found at 440 and 720 nm, indicating a common dynamics: twisting of **1b**. The inset of Figure 3B shows that, at 440 and 720 nm and larger-time window of observation, the signal is dominated by emission from the same structure with long lifetime.

To correlate the femtosecond emission to the femtosecond absorption data, Figure 4 presents a direct comparison of

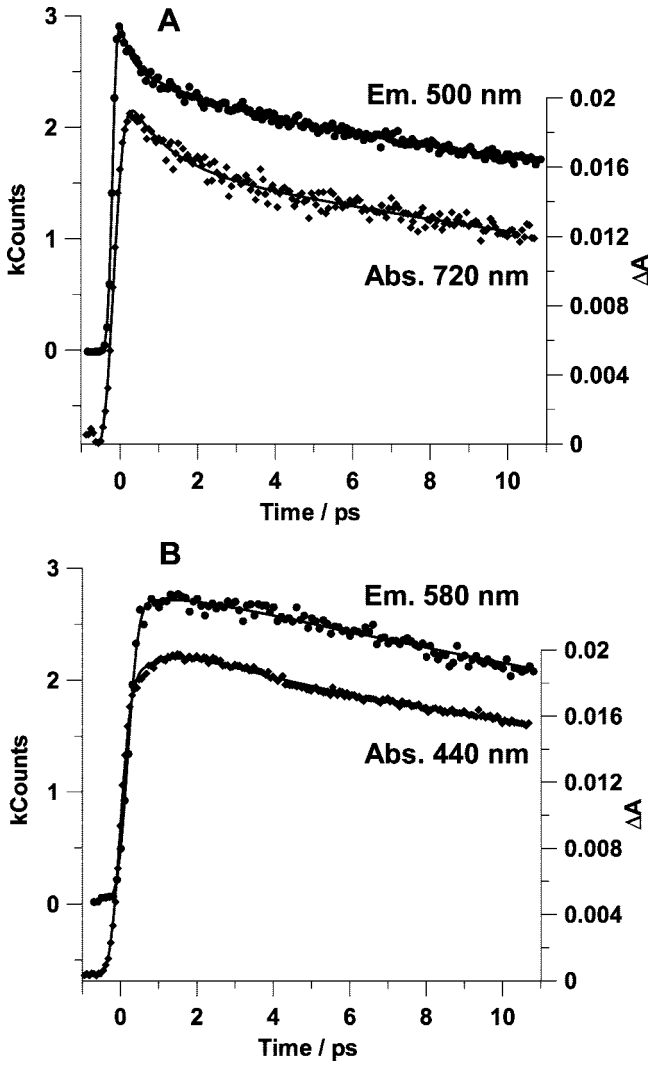

Figure 4. Comparison of femtosecond emission and transient absorption kinetic traces of **1** in THF at (A) 500 nm (emission) and 720 nm (absorption) and (B) 580 nm (emission) and 440 nm (absorption). The excitation was at 377 and 267 nm for femtosecond emission and transient absorption, respectively.

emission and absorption transients at corresponding wavelengths of observation. The fast picosecond decaying component observed in emission signal around 500 nm (Figure 4A) has its counterpart in the transient absorption around 720 nm. This clearly shows the same dynamics interrogated by both techniques but in different ways to reflect a twisting in **1b** to create keto rotamers. Moreover, the gating of these twisted structures formation is also well illustrated by the transients gated at ~580 nm in emission and at 440 nm in absorption, where a common rising component is reflected. Thus, both techniques give the time scale for the production of keto rotamers of **1b** in THF. Because of the similarity of the time constants, the shapes of the absorption and emission transients suggest not very different relative contributions of the related structures in both signals, and therefore the cross sections for absorption (from S_1 to S_2) and emission (from S_1 to S_0) are comparable. As the upconversion signal is reflecting the populations of bright states and taking into account the similar shape of 500/720 and 580/440 signals within the observed time window, the transient absorption is not gating any dark states.

In ACN (a more polar solvent than THF), the lifetime of relaxed keto rotamers is 27 ps in comparison with 42 ps in THF

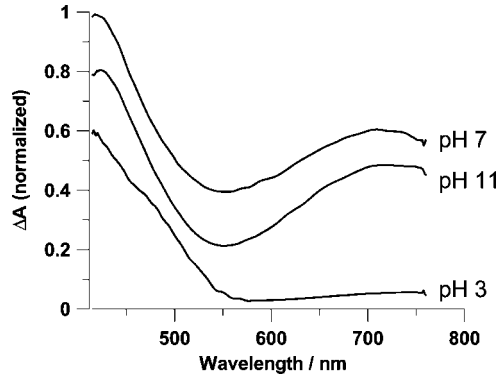

Figure 5. Normalized transient absorption spectra of **1** in water solutions at different pH values. The transients were observed at 3 ps delay after excitation at 400 nm, and for clarity they are shifted vertically.

(Table 2). The shortening is very similar to previously observed for milrinone, a cardiotonic drug that exhibits a twisting of pyridyl moiety.[30,31] This suggests that the main nonradiative process in keto rotamers due to twisting motion is possibly enhanced by an intramolecular charge-transfer (ICT) reaction (vide infra). The shortest component in the transient absorption decay in ACN has a time constant of 0.5 ps, shorter than the 1 ps observed in THF. This component is present at 720 nm as a decay and at 440 nm as a rise. It corresponds to the decaying and rising components obtained in THF, and it reflects a very fast twisting, probably coupled to fast ICT reaction. The intermediate time constant (~3 ps), which is present at the blue side of the transient band (390 nm) and assigned to VR/cooling, remains the same like in THF. This result is expected for components related to VR/cooling processes in solvents having comparable heat capacities and viscosities (η_{298K} = 0.37 cP (ACN), 0.46 cP (THF)).

3.4. Femtosecond Time-Resolved Absorption in Water. As mentioned earlier, in protic solvents the steady-state spectral behavior of **1** is quite different from that found in aprotic ones. In contrast, the transient absorption spectra collected in neutral, alkaline, and acidic water (Figure 5) are not very different from those found in THF. At the three studied pH values, the transient spectra are very broad and a stimulated emission is overlapping the absorption in the center of the examined region. The position of the maximum of stimulated emission is nearly identical in neutral and basic solution (~550 nm), but it shows some red shift in the case of acidic water (~575 nm). Also, the intensity of the low-energy part of the transient spectrum at pH = 3 is very low in comparison with other pH values. This suggests a different dominating form of **1** at pH 3 than that acting at pH = 7 and 11 and different absorbing structures at the S_1 state. The time-domain measurements give support to this suggestion and reveal much shorter decays in water at three different pH values than in THF and ACN.

3.4.1. Femtosecond Observations in Neutral and Alkaline Water Solutions. At pH = 7, two components are present in the transients (Figure 6 and Table 3). The longest component has times of 3.7 and 4.8 ps at 720 and 440 nm of observation, respectively. It is assigned to the lifetimes of the involved structures at S_1 state. The observed substantial shortening of the lifetime in water in comparison with aprotic media is due to the different structures of the formed anions **1c** (after giving a proton to the molecules of water at the ground state). Thus, we assigned this component to the lifetime of anionic forms of **1**, which are the main structures at this pH. The subpicosecond components appearing as a decay at 720 nm and as a rise at

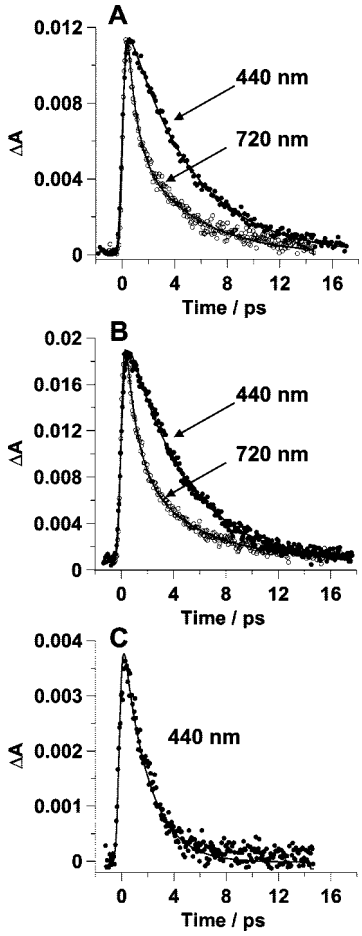

Figure 6. Transient absorption decays of **1** in water at pH = (A) 7, (B) 11, and (C) 3 and gated at 440 (●) and 720 nm (○). The solid lines are multiexponential fits of the experimental data (Table 3).

TABLE 3: Time Constants and Normalized (to 1) Pre-exponential Factors (in Parentheses, a Negative Value Indicates a Rising Component) of the Transient Absorption Decays of 1 in Water at Different pH Values[a]

	λ_{probe} = 440 nm		λ_{probe} = 720 nm	
pH = 3	2.0 ps (1.0)		<200 fs	
pH = 7	0.3 ps (−0.40)	4.8 ps (0.60)	0.3 ps (0.60)	3.7 ps (0.40)
pH = 11	0.3 ps (−0.56)	4.6 ps (0.44)	0.3 ps (0.44)	3.9 ps (0.54)

[a] The wavelengths of observation were 440 and 720 nm, and the pumping was at 400 nm.

440 nm give times of 0.3 ± 0.1 ps. We obtained a similar value for decay and rising times when using a shorter IRF of 380 fs. These times reflect the dynamics of the same event, and because of the nature of the electronic structure of the ions, we assign it to a charge-transfer process in these structures to give a charge-transferred anion (CT-1c), as happens in comparable systems.[30,32] The 4.8 ps is the lifetime of CT-1c. In milrinone, the femtosecond emission experiments show that an ICT reaction occurs in the anionic form of the medicine in ∼1.2 ps.[32] This time is longer than that in **1c**, suggesting a lower energy barrier of the ICT reaction in the former.

An increase in pH value from 7 to 11 does not significantly change the transient absorption spectra and related decays (Figure 6), supporting the assignment of the above dynamics to anions. The time values of the shorter and longer components are very similar when comparing them in solutions at pH = 7 and 11 (Table 2), but we observed some differences of the amplitudes (Table 3). We interpret this difference in terms of more efficient ICT reaction in **1c** in alkaline water than in neutral water, most probably due to a larger polarity of the former. This difference explains the red shift of the steady-state emission spectrum at pH = 11 when compared to that observed at pH = 7.

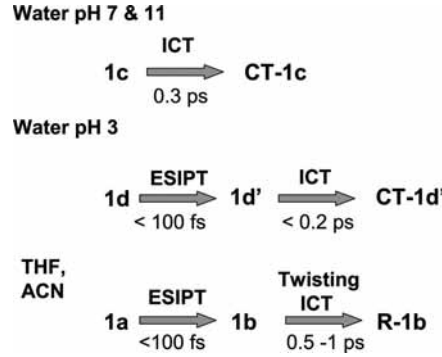

Figure 7. Schematic representation of the involved structures and times in the ultrafast dynamics of **1** in water solutions and in THF (ACN). For the identification of the structures, see Figure 1 and discussion in the text. ICT and R denote intramolecular charge transfer and rotamer/twisted structures, respectively.

3.4.2. Femtosecond Observations in Acidic Water Solution. In water at pH = 3, the transient signal is weak because of low solubility of **1** in this medium. However, we measured a transient absorption spectrum and decay with good confidence at the maximum of intensity (∼440 nm) (Figure 6). The analysis of this transient gives a monoexponential decay of 2 ps (Table 2). We assigned this time constant to the lifetime of a keto cation form (**1d′**). Therefore, upon excitation of a cation structure **1d**, an ultrafast ESIPT reaction takes place to produce a cationic keto form **1d′**, having still a proton on the nitrogen atom of the pyridinium moiety. Because of protonation, an ultrafast ICT reaction in this structure should take place. We observed a very weak transient band at 720 nm, contrary to the situation in neutral and alkaline water, and organic solvents. This observation supports the assignment of the 720-nm band to a structure undergoing an ultrafast ICT reaction (<200 fs). Because of the involvement of the (n,π^*) state, caused by the protonation of the nitrogen atom, fast crossing to the PES of these state occurs, leading to a very short lifetime of the cationic keto form. The ICT reaction here is faster than that for cationic species of milrinone, where it takes ∼0.6 ps to form an excited ICT structure by charge migration to the protonated pyridinium ring.[32] In the present case, an enhanced charge migration induced by the cationic pyridinium moiety is more favorable in the cationic keto species. It explains the weak absorption signal of an extremely short-living state (<200 fs) around 700 nm. Notice that theoretical studies of several ESIPT-capable molecules show that interaction of PES of an optically excited ($^1\pi,\pi^*$) state with a closely lying dark (^{1}n,π^*) state plays an important role in the increase of a nonradiative rate constant. A mixing of these states is accessible through a vibronic coupling, and it is sensitive to the polarity and H-bond donating ability of the solvent.[33−36] A very fast step for deactivation is a conical intersection occurring by a crossing of PES of excited and ground states. Figure 7 shows the involved times and molecular structures of **1** in water solutions at different pHs and in an aprotic solvent.

4. Conclusions

In this contribution, using two ultrafast techniques we showed strong interactions of different structures of **1** with water at both

ground and electronic excited states. The similar dynamics observed in neutral and alkaline water solutions confirm that the anionic structure is the predominant form of **1** in a physiological pH medium. The formation of charge-transfer structure occurs in 0.3 (±0.1) ps and their relaxation to the ground state in 3.7−4.8 ps. In acidic water, the excited cation shows an ESIPT reaction and a very fast ICT reaction in the formed structure (<0.2 ps), reflecting a strong interaction with the medium. The subsequent relaxation to ground state occurs in 2 ps. In contrast to the behavior in water solutions, the interactions of neutral **1** with organic solvents are different. It is reflected in a slower twisting motion to give a rotamer of its keto-formed tautomer. These differences can have additional consequences when considering a biologically relevant nanoenvironment or a nanocarrier, where confinement and electrostatic interactions may shape the structure of **1**. In a hydrophobic pocket such as those of human serum albumin protein, the drug will encounter a rather different surrounding than in bulk water. Since only the neutral forms of the oxicam family drugs are supposed to cross the blood−brain barrier, the findings of this work could be useful for further pharmaceutical and medical research.

Acknowledgment. This work was supported by the JCCM and MEC through projects PCI08-0037-5868, CTQ-2005-00114/BQU, and UNCM05-23-034.

Supporting Information Available: Figure S1 shows the femtosecond emission decays in THF at different wavelengths of observation. Figure S2 provides comparison of femtosecond emission transients in THF upon excitation at 377 and 261 nm, while Table S1 gives times and amplitudes obtained for higher excited decays. Figure S3 presents transient absorption spectra in THF. This material is available free of charge via the Internet at http://pubs.acs.org.

References and Notes

(1) Pal, S. K.; Zhao, L.; Zewail, A. H. *Proc. Natl. Acad. Sci. U.S.A.* **2003**, *100*, 8113.

(2) Qu, X.; Wan, C.; Becker, H.-C.; Zhong, D.; Zewail, A. H. *Proc. Natl. Acad. Sci. U.S.A.* **2001**, *98*, 14212.

(3) Zhong, D.; Pal, S. K.; Wan, C.; Zewail, A. H. *Proc. Natl. Acad. Sci. U.S.A.* **2001**, *98*, 11873.

(4) El-Kemary, M.; Organero, J. A.; Santos, L.; Douhal, A. *J. Phys. Chem. B* **2006**, *110*, 14128.

(5) Lillo, M. P.; Canadas, O.; Dale, R. E.; Acuña, A. U. *Biochemistry* **2002**, *41*, 12436.

(6) Shen, Y.; Myslinski, P.; Treszczanowicz, T.; Liu, Y.; Koningstein, J. A. *J. Phys. Chem.* **1992**, *96*, 7782.

(7) Monti, S.; Manet, I.; Manoli, F.; Sortino, S. *Photochem. Photobiol. Sci.* **2007**, *6*, 462.

(8) Marconi, G.; Monti, S.; Manoli, F.; Degli Esposti, A.; Mayer, B. *Chem. Phys. Lett.* **2004**, *383*, 566.

(9) Chergui, M. *Chem. Phys. Chem.* **2002**, *3*, 713.

(10) Zewail, A. H. *Angew. Chem., Int. Ed.* **2000**, *39*, 2586.

(11) Diffey, B. L.; Daymond, T. J.; Fairgreaves, H. *Br. J. Rheumatol.* **1983**, *22*, 239.

(12) Serrano, G.; Bonillo, J.; Aliaga, A.; Gargallo, E.; Pelufo, C. *J. Am. Acad. Dermatol.* **1984**, *11*, 113.

(13) Tsai, R.-S.; Carrupt, P.-A.; El-Tayar, N.; Giroud, Y.; Andrade, P.; Testa, B.; Bree, F.; Tillement, J.-P. *Helv. Chim. Acta* **1993**, *76*, 842.

(14) Bordner, J.; Hammen, P. D.; Whipple, E. B. *J. Am. Chem. Soc.* **1989**, *111*, 6572.

(15) Yoon, M.; Choi, H. N.; Kwon, H. W.; Park, K. H. *Bull. Korean Chem. Soc.* **1988**, *9*, 171.

(16) Banerjee, R.; Sarkar, M. *J. Lumin.* **2002**, *99*, 255.

(17) Kim, Y. H.; Cho, D. W.; Kang, S. G.; Yoon, M.; Kim, D. *J. Lumin.* **1994**, *59*, 209.

(18) Cho, D. W.; Kang, S. G.; Kim, Y. H.; Yoon, M.; Kim, D. *J. Photosci.* **1994**, *1*, 15.

(19) Andrade, S. M.; Costa, S. M. B. *Phys. Chem. Chem. Phys.* **1999**, *1*, 4213.

(20) Andrade, S. M.; Costa, S. M. B. *Prog. Colloid Polym. Sci.* **1996**, *100*, 195.

(21) Andrade, S. M.; Costa, S. M. B.; Pansu, R. *Photochem. Photobiol.* **2000**, *71*, 405.

(22) El-Kemary, M.; Gil, M.; Douhal, A. *J. Med. Chem.* **2007**, *50*, 2896.

(23) Banerjee, R.; Chakraborty, H.; Sarkar, M. *Biopolymers* **2004**, *75*, 355.

(24) Andrade, S. M.; Costa, S. M. B.; Pansu, R. *J. Colloid Interface Sci.* **2000**, *226*, 260.

(25) Oyekan, A. O.; Thomas, W. O. A. *J. Pharm. Pharmacol.* **1984**, *36*, 831.

(26) Bree, F.; Urien, S.; Nguyen, P.; Albengres, E.; Tillement, J. P. *Eur. J. Metab. Pharmacokinet.* **1990**, *15*, 303.

(27) Cho, D. W.; Kim, Y. H.; Yoon, M.; Jeoung, S. C.; Kim, D. *Chem. Phys. Lett.* **1994**, *226*, 275.

(28) Gil, M.; Douhal, A. *Chem. Phys.* **2008**, *350*, 179.

(29) Becker, R. S.; Chakravorti, S.; Yoon, M. *Photochem. Photobiol.* **1990**, *51*, 151.

(30) Gil, M.; Douhal, A. *Chem. Phys. Lett.* **2006**, *428*, 174.

(31) El-Kemary, M.; Organero, J. A.; Douhal, A. *J. Photochem. Photobiol., A* **2007**, *187*, 339.

(32) Gil, M.; Douhal, A. *Chem. Phys. Lett.* **2006**, *432*, 106.

(33) Sobolewski, A. L.; Domcke, W.; Hättig, C. *J. Phys. Chem. A* **2006**, *110*, 6301.

(34) Sobolewski, A. L.; Domcke, W. *Phys. Chem. Chem. Phys.* **2006**, *8*, 3410.

(35) Chachisvilis, M.; Zewail, A. H. *J. Phys. Chem. A* **1999**, *103*, 7408.

(36) Blancafort, L.; Cohen, B.; Hare, P. M.; Kohler, B.; Robb, M. A. *J. Phys. Chem. A* **2005**, *109*, 4431.

JP803457E